

Towards Better Benchmark Datasets for Inductive Knowledge Graph Completion

Harry Shomer
Michigan State University
East Lansing, USA
shomerha@msu.edu

Jay Revolinsky
Michigan State University
East Lansing, USA
revolins@msu.edu

Jiliang Tang
Michigan State University
East Lansing, USA
tangjili@msu.edu

Abstract

Knowledge Graph Completion (KGC) attempts to predict missing facts in a Knowledge Graph (KG). Recently, there’s been an increased focus on designing KGC methods that can excel in the *inductive setting*, where a portion or all of the entities and relations seen in inference are unobserved during training. Numerous benchmark datasets have been proposed for inductive KGC, all of which are subsets of existing KGs used for transductive KGC. However, we find that the current procedure for constructing inductive KGC datasets inadvertently creates a shortcut that can be exploited even while disregarding the relational information. Specifically, we observe that the Personalized PageRank (PPR) score can achieve strong or near SOTA performance on most datasets. In this paper, we study the root cause of this problem. Using these insights, we propose an alternative strategy for constructing inductive KGC datasets that helps mitigate the PPR shortcut. We then benchmark multiple popular methods using the newly constructed datasets and analyze their performance. The new benchmark datasets help promote a better understanding of the capabilities and challenges of inductive KGC by removing any shortcuts that obfuscate performance. The code and dataset can be found <https://github.com/HarryShomer/Better-Inductive-KGC>.

CCS Concepts

• Computing methodologies → Machine learning.

Keywords

Knowledge graphs, Link prediction

ACM Reference Format:

Harry Shomer, Jay Revolinsky, and Jiliang Tang. 2025. Towards Better Benchmark Datasets for Inductive Knowledge Graph Completion. In *Proceedings of the 31st ACM SIGKDD Conference on Knowledge Discovery and Data Mining V.2 (KDD ’25)*, August 3–7, 2025, Toronto, ON, Canada. ACM, New York, NY, USA, 14 pages. <https://doi.org/10.1145/3711896.3737438>

1 Introduction

Knowledge Graph Completion (KGC) attempts to predict unseen facts given an existing knowledge graph (KG). KGC has numerous applications including drug discovery [40], personalized medicine [5], and recommendations [36]. Traditionally, most research on KGC was focused on the transductive setting, where the same sets of

entities and relations are seen during training and testing. Most methods [4, 28, 35] generally focus on learning embeddings for all entities and relations to facilitate the prediction of new facts.

In recent years, interest in KGC has shifted towards designing methods that can generalize to new entities or relations not seen during training. This task, known as “inductive KGC”, requires a method to train on a graph $\mathcal{G}_{\text{train}}$ and perform inference on a different graph \mathcal{G}_{inf} , where the inference graph contains either new entities, relations, or both. Because of this, methods for inductive KGC don’t rely on fixed embeddings for entities or relations, instead opting for more flexible techniques that can inductively learn representations based on a given graph [20, 33, 44]. To assess the ability of methods for this task, new datasets have been constructed that require methods to reason inductively. All inductive datasets [12, 20, 33] are constructed from existing transductive KGC datasets. This is done by sampling two graphs, one each for train and inference, which contain disjoint entities. Multiple methods [20, 41, 44] have reported tremendous promise on these newer benchmark datasets.

However, we find that on almost all inductive datasets, we can achieve competitive performance by using the Personalized PageRank (PPR) score [24] to perform inference. We note that PPR is a non-learnable heuristic and ignores the relational information in the graph. In Figure 1, we compare the performance of PPR against the supervised SOTA performance on both inductive and transductive datasets. We can see that when performing KGC on inference graphs with either new entities (E) or new entities and relations (E, R), PPR performs only roughly 25% worse than SOTA. However, this is generally not true for transductive datasets, where PPR usually performs poorly. Interestingly, this observation is true for inductive datasets even when the transductive dataset that it is created from has poor PPR performance. For example, while PPR performs very poorly on FB15k-237, it achieves higher performance on its inductive derivatives (denoted by “FB”). These findings are problematic as PPR has no basis in literature as a heuristic for KGC, since it completely overlooks the relational aspect of KGs. Therefore, this suggests the potential existence of a shortcut that allows a simple non-learnable method like PPR to achieve high performance on almost all inductive datasets. This also brings into question how successful most methods are in inductive reasoning, as a large portion of their performance may be due to this shortcut.

This finding naturally motivates us to ask – *why can PPR perform so well on existing inductive datasets?* In Section 3 we discover that the high performance of PPR is due to how the inductive datasets are created from transductive datasets. Specifically, we observe that the current procedure creates graphs where the shortest path



This work is licensed under a Creative Commons Attribution 4.0 International License. *KDD ’25, Toronto, ON, Canada*

© 2025 Copyright held by the owner/author(s).
ACM ISBN 979-8-4007-1454-2/2025/08
<https://doi.org/10.1145/3711896.3737438>

distance (SPD) between entities in positive test samples is much lower than the SPD between those in negative samples. This allows for a method like PPR, which gives a higher weight to shorter walks, to distinguish between the positive and negative samples based solely on the distance. To account for this problem, in Section 4 we propose a new strategy for sampling inductive datasets that uses graph partitioning to create the train and inference graphs. This allows us to sample subgraphs that retain the general properties of the original graph. We then demonstrate that this procedure can indeed create inductive datasets that greatly mitigates the ability of PPR. Lastly, we benchmark common inductive KGC methods on our newly constructed datasets. Our key contributions can be summarized as follows:

- We observe that on existing inductive KGC datasets, we can achieve competitive performance when ranking entities using only the Personalized PageRank score.
- Through empirical study, we find that the strong performance of PPR on inductive datasets is due to the current procedure for constructing inductive datasets, which allows for a shortcut to distinguish between positive and negative samples.
- We propose a new strategy for sampling inductive KGC datasets from their transductive counterparts that uses graph partitioning. We show that our proposed method can substantially mitigate the shortcut. We then benchmark popular methods on our newly created datasets. Compared to the older datasets, methods tend to decrease in performance.

The remaining paper is structured as follows. In Section 2, we provide background on inductive KGC methods and datasets and PPR. In Section 3, we study in detail when and why PPR can perform well on inductive KGC. We then introduce our new strategy for creating inductive datasets in Section 4 and benchmark popular methods on these newly created datasets in Section 5.

2 Background and Related Work

Throughout this study we denote a knowledge graph as $\mathcal{G} = \{\mathcal{V}, \mathcal{R}, \mathcal{E}\}$ where \mathcal{V} are the set of entities (i.e., nodes), \mathcal{R} the set of relations (i.e., edge types), and \mathcal{E} the set of edges (i.e., triples) of the form (s, r, o) where s and o are entities and r a relation. Lastly, we note that the task of KGC is formulated as the following where given a query $(s, r, *)$, we attempt to predict the correct entity $*$.

Inductive KGC Datasets: In inductive KGC, we are given a training graph $\mathcal{G}_{\text{train}} = \{\mathcal{V}_{\text{train}}, \mathcal{R}_{\text{train}}, \mathcal{E}_{\text{train}}\}$ and an inference graph $\mathcal{G}_{\text{inf}} = \{\mathcal{V}_{\text{inf}}, \mathcal{R}_{\text{inf}}, \mathcal{E}_{\text{inf}}\}$. A method is trained on $\mathcal{G}_{\text{train}}$ and evaluated on \mathcal{G}_{inf} . Most datasets consider the setting that is only disjoint on the entities such that $\mathcal{R}_{\text{inf}} \subseteq \mathcal{R}_{\text{train}}$ and $\mathcal{E}_{\text{inf}} \cap \mathcal{E}_{\text{train}} = \emptyset$. This setting is referred to as the **(E) setting**. Another setting, which we denote as **(E, R)** further allows \mathcal{R}_{inf} to contain relations not in $\mathcal{R}_{\text{train}}$.

All existing inductive datasets are sampled from existing transductive datasets. Furthermore, the majority of inductive datasets [20, 33] are further created via the same procedure introduced by [33]. We now give a brief overview of this procedure. Given a transductive dataset, which we denote as \mathcal{G} , k seed entities are randomly chosen from \mathcal{G} . The 2-hop neighborhood is then extracted around each individual seed entity. To prevent exponential growth, the number of neighbors sampled at any hop is capped at 50 for each

seed entity. The resulting edges are then combined to create $\mathcal{G}_{\text{train}}$ and are subsequently removed from the original graph. The inference graph is then sampled in a similar manner from the resulting graph $\mathcal{G} \setminus \mathcal{G}_{\text{train}}$. One exception to this procedure are the ILPC datasets, introduced by [12], which instead sample $p\%$ of the nodes from \mathcal{G} and use them to create $\mathcal{G}_{\text{train}}$. The rest of the nodes are then used to construct \mathcal{G}_{inf} . In practice, we find that both methods tend to produce similar graphs.

Inductive KGC Methods: NeuILP [39] and DRUM [26] consider combining the path representations of different length between both entities in a triple. However, since they explicitly consider each path, they are often limited to only considering paths of up to length 2 or 3. Conditional MPNNs [19] are a more efficient alternative to encoding higher-order path information. They work by conditioning the message passing mechanism on the known entity, allowing the implicit aggregation of all paths up to a length L (which is equal to the number of GNN layers). The value of L is typically 5 or 6. Prominent examples include NBFNet [44] and RED-GNN [41]. More scalable alternatives have been proposed that prune the propagated messages [31, 42, 43]. NodePiece [13] is concerned with parameter efficiency, using an anchor-based approach to learn a more compact set of entity and relation representations. All previous methods assume that a fixed set of relations exist between the train and inference graphs. To account for new relations in inference, InGRAM [20] introduces the concept of a “relation graph”, which inductively encodes the representation of each relation. Gao et al. [15] introduces the concept of “double permutation-equivariant representations” as a way to model KGs that are equivariant to permutations of both the entities and relations. They theoretically show that capturing this property is essential for proper generalization across KGs. To this point these introduce a new method, ISDEA/ISDEA+, that can satisfy this property. They further introduce a variant of InGRAM [20], DEq-InGram, that endows it with the ability to compute double equivariant representations. Note that we omit subgraph methods that have been shown to prohibitively expensive [16, 21, 23, 33, 38] or those that require the use of external textual information [8, 17].

Personalized PageRank: PageRank [24] computes the probability of finishing a random walk of arbitrary length at some node u , when there is equal probability of beginning the walk at any node in the graph. Personalized PageRank (PPR) [24] is a version of PageRank that is “personalized” to some root node s , where at each step there is a probability α of teleporting to s . The set of PPR scores for a root node s is given by $\text{pr}_s \in \mathbb{R}^{|\mathcal{V}|}$ and can be formulated as the weighted sum of all random walk probabilities between two nodes [7]:

$$\text{pr}_s = \alpha \sum_{k=0}^{\infty} (1 - \alpha)^k W^k x_s, \quad (1)$$

where $W = D^{-1}A$ and x_s is a one-hot vector at node s . Observe that the weight given to a walk decays with the increase in length due to $(1 - \alpha)^k$. As such, the PPR score will often be higher for those nodes of shorter distance to s . For a KG, we obtain the PPR matrix by first converting the inference graph, \mathcal{G}_{inf} , to an undirected graph. This is common practice in KGC [9] whereby inverse relations are added to the graph. We further assume an edge weight of 1 for all edges.

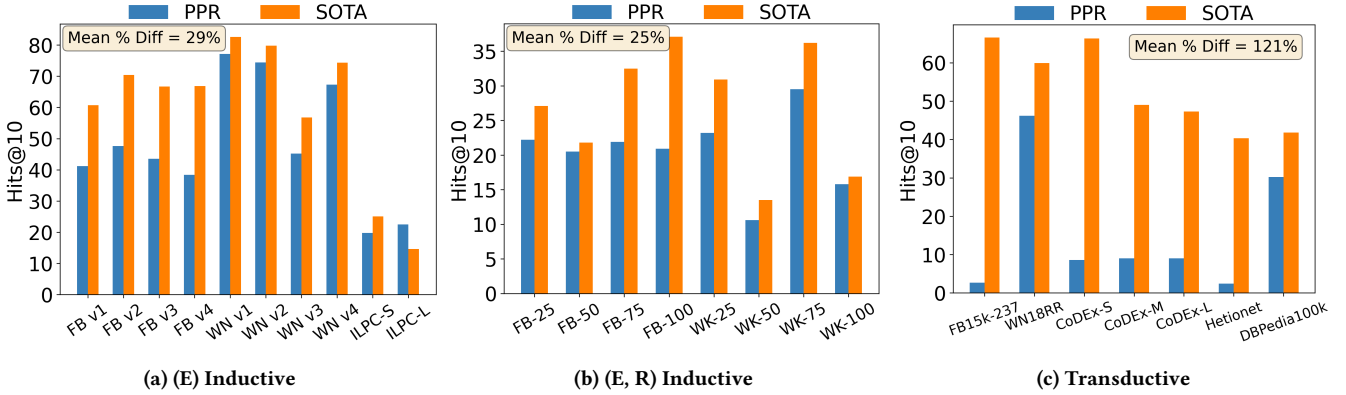


Figure 1: Hits@10 of PPR vs. Supervised SOTA. Results are on (a) (E) Inductive, (b) (E, R) Inductive, and (c) Transductive datasets.

As such, the relations are completely disregarded when computing the PPR.

3 Preliminary Study

In this section, we examine the performance on common inductive KGC datasets. We first show that the Personalized PageRank (PPR) can often serve as a good baseline on most datasets. From this observation, we attempt to answer two important questions: (1) When can the PPR scores perform well on KGC? and (2) Why can PPR sometimes perform well for KGC?

3.1 Personalized Pagerank (PPR) is a Strong Baseline for Inductive KGC

We begin by obtaining the PPR matrix of the inference graph for use in evaluation. See Section 2 for more details on how this is done. Given this new graph, for a query $(s, r, *)$, we calculate the PPR score for all possible entities $o \in \mathcal{V}$. Using these scores, we can obtain the rank of the true entity for our query. We emphasize that PPR is (a) a non-learnable heuristic, (b) ignores the relations in the KG, and (c) has no basis in KG literature as a method to perform KGC.

In Figure 1, we show the performance when using the PPR versus the SOTA performance among supervised methods. The SOTA method is dataset dependent, with the specific methods are shown in Appendix A.1.. We split the datasets by transductive, (E), and (E, R) inductive. We include those datasets most often used in each task, comprising 25 in total. Please see Appendix B.1 for more on the datasets chosen. The full set of results are shown in Table 6.

We observe that on both types of inductive datasets, the PPR score does reasonably well, **performing on average only 25-29% less than SOTA**. This is surprising as PPR is both non-learnable and ignores the relations of the KG. We also find that on some datasets like the WN or ILPC inductive splits, the performance nearly matches or exceeds the supervised performance. On the other hand, for the transductive datasets, the performance disparity is often much larger. Interestingly, we note that PPR still performs well on some transductive datasets, including the popular WN18RR. This tells us that this phenomenon is not necessarily unique to inductive datasets, but is most apparent there.

Furthermore, we find that for the inductive datasets, their PPR performance is much higher than their transductive parents. We detail this in Figure 2a where for different inductive datasets we see the percent increase in PPR performance from transductive to inductive. For example, on FB15k-237 the PPR Hits@10 is 2.7%, however the mean performance on the four FB (E) splits is 42.7%, representing a 1481% increase. We can see that the % increase on each inductive dataset is large, with the smallest being 42% on WN. This suggests that there is some change in the underlying inductive graphs that are causing the performance of PPR to increase. Lastly, we further explore other potential shortcuts in Appendix A.4, finding that PPR is by far the most severe.

3.2 When Does PPR Perform Well and Why?

In the previous section we detailed that PPR score performs well on the inductive setting. Furthermore, the performance of PPR on inductive datasets is much higher than their transductive counterparts of which they’re derived from. This raises the question – *why can PPR perform well on some datasets but not others?*

We find that the answer lies in **comparing the mean shortest path distance (SPD) between positive and negative samples**. For a query $(s, r, *)$, let’s denote o^+ as the correct answer and $o^- \in \mathcal{V}^-(s, r)$ as the set of negative answers for the query. We compute the SPD on the inference graph for both the o^+ and $\mathcal{V}^-(s, r)$. This is repeated for each test sample $(s, q, *) \in \mathcal{E}_{\text{inf}}$. We then calculate the mean SPD across all positive and negative test samples, which we denote as SPD^+ and SPD^- , respectively. The difference in mean SPD is correspondingly given by $\Delta\text{SPD} = \text{SPD}^- - \text{SPD}^+$. This tells us, on average, how much shorter the distance between entities in positive samples are relative to those in negatives.

In Figure 2b we show the relationship between ΔSPD and the Hits@10 when using PPR. The results are across 25 different datasets, for both inductive and transductive KGC. Calculating the Pearson correlation, we can observe it is 0.87, which indicates a strong relationship between the two metrics. Therefore, there exists a basic pattern to distinguish positive and negative samples in many KGC datasets. Put simply, the SPD between entities in positive test samples tend to be lower than that in negative samples. The larger the

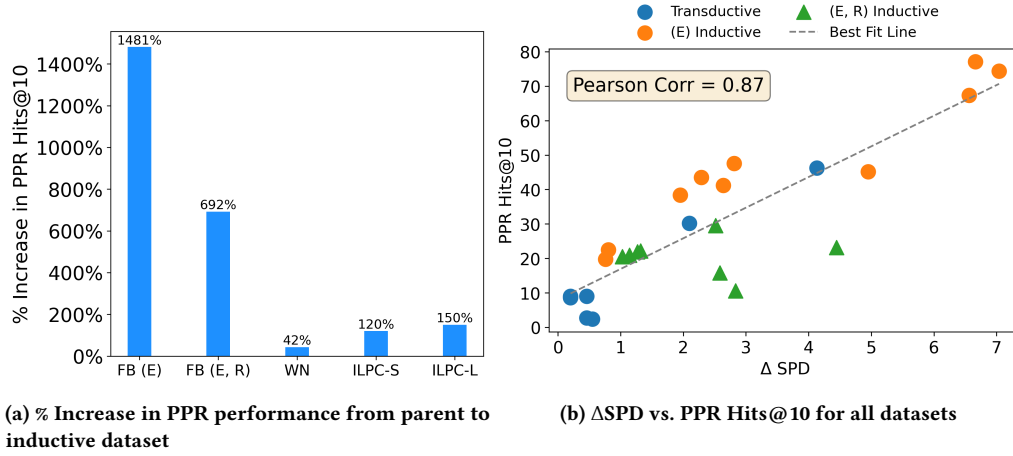


Figure 2: (a) Percent increase in PPR performance on the inductive datasets as compared to their parent transductive dataset. For datasets with multiple splits (i.e., FB and WN) we take the mean performance across each. (b) Relationship between Δ SPD and performance. We observe a strong relationship among both transductive and inductive datasets.

discrepancy between the mean distances, the better PPR can perform. This suggests that the PPR scores can exploit this pattern in the datasets, to achieve good performance, even while completely ignoring the relation information.

But, why can PPR exploit this pattern? As shown in Eq. (1), the PPR score between two nodes is the weighted sum of walks between them. Furthermore, walks of shorter length are weighed more heavily than those of longer length. Therefore, nodes with a shorter distance between them will be able to benefit from these highly-weighted walks, while those of larger distance will not. For example, when $\alpha = 0.15$, the highest weight for a walk when $\text{SPD} = 2$ is 0.72 while when $\text{SPD} = 5$ it is 0.44. As such, the PPR score will invariably favor those node pairs with a lower SPD.

Table 1: % Increase in Positive vs. Negative sample PPR, broken down by SPD.

SPD	WN18RR v4	FB15k-237 v4
[1, 2)	+17%	+5%
[2, 3)	+29%	+200%
[3, 4)	+82%	+328%
[4, ∞)	+2837%	+44%

Note that we use PPR as opposed to SPD in our experiments since all-pairs SPD is costly to calculate and the full PPR matrix can be efficiently approximated via [2]. Furthermore, as we show in Section 3.3, even when controlling for the SPD, the PPR score can help differentiate between positive and negative samples.

3.3 Why is This So Common on Inductive Datasets?

In the last section, we covered when PPR can perform well on KGC and why. However, one remaining question is – *why is this trend so pervasive on inductive datasets but rarely on their transductive*

counterparts? For example, on FB15k-237, a transductive dataset, the Hits@10 of PPR is 2.7%. However, across eight different inductive versions of FB15k-237, the mean PPR performance is 32%. We find that this can be explained by the following two observations.

Observation 1: The current procedure for creating inductive datasets increases the Δ SPD and thereby the performance of PPR. As noted earlier, all common inductive datasets are created from existing transductive datasets. See Section 2 for a detailed overview of the construction process. In a nutshell, the training and inference graph are constructed sequentially by sampling a number of subgraphs from a graph. In Figure 3 we show the mean SPD of both positive and negative samples for 12 inductive datasets and their parent transductive dataset. We limit our analysis to those datasets derived from FB15k-237 and WN18RR, as the majority of inductive datasets are derived from them. We observe that for all inductive datasets, while the mean SPD for negative samples sharply rises, the mean SPD for positive samples stay roughly the same. This creates the shortcut described in Section 3.2, where the SPD can easily differentiate between positive and negative samples. Since the gap between the distances is almost always larger than the original transductive dataset, this shortcut becomes more pronounced, thereby leading to a better PPR performance.

But why does the mean SPD drastically change for negative samples but not positive? We find that entities in positive samples are more well-connected than those in negatives. In Table 1, we show the % difference in PPR score between positive and negative samples when controlling for the SPD on two inductive datasets.

We can see that the PPR score is much greater for positive samples, even for higher values of SPD. Therefore, the SPD of positive samples are better able to “withstand” changes in the underlying graph better than negatives, as they typically contain additional shorter walks between samples. However, negatives are typically much less well-connected, so they are more affected by removing a portion of edges from the original graph.

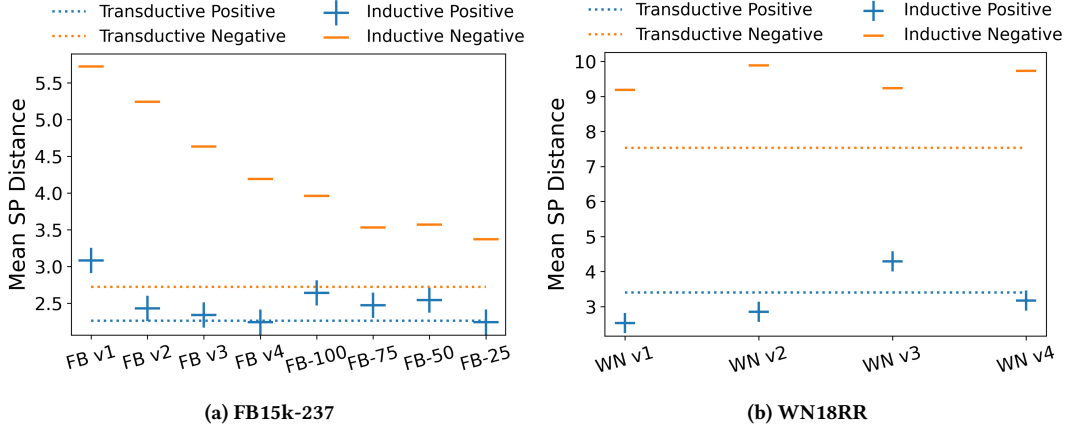


Figure 3: The mean shortest path (SP) distance between positive test samples and negative samples. We display the results for two transductive datasets (FB15k-237 and WN18RR) and the inductive datasets that are derived from them.

Observation 2: Constructing a good inductive dataset is difficult. In Section 2 we discuss the general algorithm used to create inductive datasets. Multiple parameters exist that guide the construction process. It is tempting to think that by simply trying different combinations, one can happen upon a split that doesn’t suffer from high PPR performance. However, in practice, we find that this is difficult, as there are multiple factors to contend with.

We demonstrate this by attempting to generate inductive datasets from FB15k-237. We generate a number of different inductive datasets by modifying the (a) # of seed entities for train and inference and (b) the maximum neighborhood size for train and inference. For different combination of values, we generate three different datasets using different random seeds. For each of the generated datasets, we calculate the size of both the train and inference graphs, the Δ SPD, and the PPR performance. These values are then averaged across seeds. A more detailed discussion is given in Appendix C. In Figure 4a we plot the Δ SPD vs. the PPR performance. Despite searching across a wide variety of parameters, both Δ SPD and the PPR performance remain much higher for the inductive datasets compared to the transductive dataset. Furthermore, we show the relationship between the size of the train and inference graphs and the PPR performance in Figures 4b and 4c. We observe that when the performance of PPR is at its lowest, the size of the train graph is noticeably small. However, fixing this problem, results in a sharp increase in the performance of PPR. Furthermore, there is an inverse relationship between the size of the train and inference graph, making it hard to find a “sweet spot” where the PPR performance is low and both graphs aren’t too small.

Discussion. The studies in this section show that the current strategy for constructing inductive datasets from existing transductive datasets is liable to introduce a well-performing shortcut into the existing graph. Currently, it almost always leads to a sharp increase in the PPR performance. Furthermore, attempting to limit the severity of this issue is very difficult while also generating train and inference graphs of reasonable sizes. **This suggests that a new**

strategy is needed for sampling graphs for inductive KGC from transductive datasets.

4 Constructing Inductive Datasets through Graph Partitioning

In the previous section, we showed that the PPR score can achieve strong performance on most inductive KGC datasets. Furthermore, we demonstrate that this is due to how inductive datasets are sampled from existing transductive datasets. This sampling strategy engenders a shift in the underlying properties of the graph that allows for PPR to perform well. This naturally causes us to ask – *How can we mitigate this problem when constructing newer inductive datasets?* In the next subsection, we introduce our strategy which utilizes graph partitioning to alleviate this problem.

4.1 Partition-Based Dataset Sampling

We’ve previously covered in Section 3 that the existing procedure for creating inductive datasets leads to suboptimal subgraphs. This is because the resulting subgraphs tend to have much different properties than the original graph, such as the distance distribution, which can potentially lead to shortcuts when performing KGC.

We note that the task of constructing inductive datasets from an existing graph \mathcal{G} can be framed as a graph partitioning problem. Formally, we want to sample two non-overlapping partitions from the graph such that $\mathcal{G}_{\text{train}}, \mathcal{G}_{\text{inf}} \subseteq \mathcal{G}$ and $\mathcal{G}_{\text{train}} \cap \mathcal{G}_{\text{inf}} = \emptyset$. Given the analysis in Section 3.2, we hope to sample subgraphs such that $\Delta\text{SPD}(\mathcal{G}_{\text{train}}) \approx \Delta\text{SPD}(\mathcal{G}_{\text{inf}}) \approx \Delta\text{SPD}(\mathcal{G})$. But, *how do we find subgraphs that satisfy this property?* Intuitively, we want to sample each subgraph so that it’s removal has little effect on the initial graph’s structure. We give an example in Figure 5 where we sample two subgraphs from an existing graph. As we can see, even though the graph is partitioned, the relationship between entities *in the same partition* remain roughly the same before and after the partition. This is because there already exists little relationship between the two partitions in the original graph.

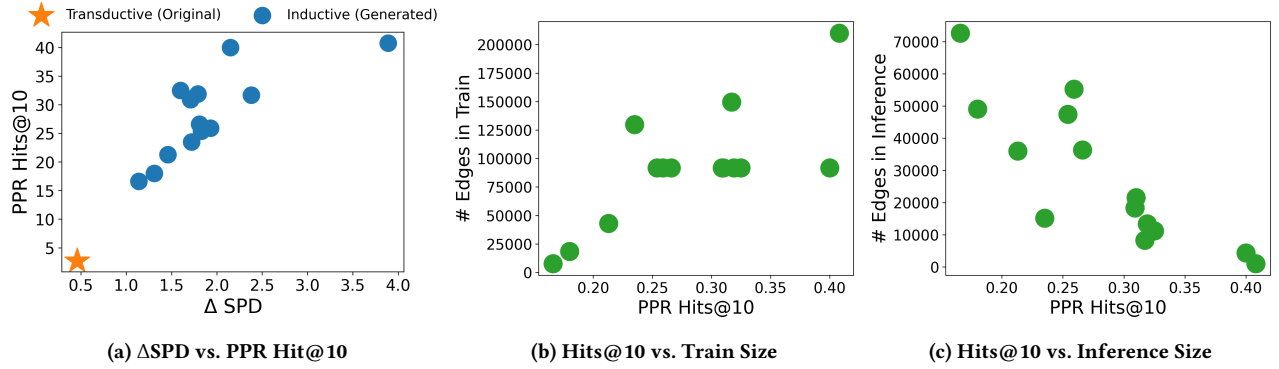


Figure 4: Experiments when generating inductive datasets from FB15k-237. (a) The generated datasets always have a much higher ΔSPD than the transductive dataset. Furthermore, there is a trade-off between the size of the train (b) and inference graph (c), making it difficult to obtain a good split.

Multiple popular approaches [3, 29] exist that attempt to divide the graph into optimal partitions. The guiding principle in these approaches is that the partitions should be internally dense but only sparsely connected to one another. Because of this, the entities in different partitions should only be weakly connected and have little impact on one another. Therefore, the relationship between entities in the same partition are minimally affected by outside entities or edges. As such, removing this partition from the graph should then have little effect on the entities in that partition. Also, since the partitions are created at the same time, we avoid sampling the inference graph after the training, which can be suboptimal.

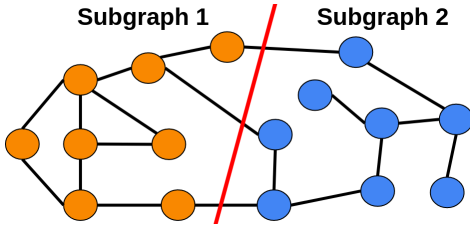


Figure 5: Sampling Two Subgraphs

In practice, we consider using Spectral Clustering [29] or the Louvain method [3], as dependent on the dataset. Once the original graph is partitioned into n partitions, we sample k of those to be used. The partitions are chosen such that they display similar properties to the original graph (see Section 4.2 for more). Of the k partitions, one is chosen as the training graph while the other $k - 1$ are designated as *separate* inference graphs. This is an important advantage of using partitioning to sample the graphs, as it allows us to avoid having to sample multiple different train and inference pairs as in [20, 33], thereby allowing for more efficient benchmarking. Lastly, we note that when sampling graphs for the (E) inductive task, we further remove new relations from the inference graph. In practice, we find that we can easily find partitions where this amounts to little or no change in the inference graph. See Section B.2 for more details on the dataset creation process.

4.2 Analysis of New Datasets

In this section we analyze the new inductive datasets created following the partition-based procedure outlined in Section 4.1. We create (E) inductive datasets, from WN18RR [9], CoDEX-M [27], and HetioNet [18]. For the (E, R) datasets, we use CoDEX-M [27] and FB15k-237 [34]. Note that some datasets are only suitable for one task or another. For example, WN18RR and HetioNet have very few relations, making it nearly impossible to sample two partitions with significantly different relations for the (E, R) task. On the other hand, FB15k-237 contains too many relations to sample multiple graphs for the (E) tasks without removing many edges from either graph.

In Table 2 we show the PPR Hits@10 and ΔSPD for the inductive datasets and their original transductive dataset. When multiple inference graphs exist, we take the mean across each inference graph. When possible, we also include a comparison against those inductive datasets that already exist. For example, for WN18RR in the (E) task, 4 datasets exist from [33]. Compared to the old inductive datasets, the PPR performance for the newer datasets is much lower. Specifically, the **average PPR performance is 78% lower on the new inductive datasets as compared to the older datasets**. Also, the PPR performance of the new inductive datasets is very similar to the performance on the original transductive dataset. A similar trend can be found when comparing the ΔSPD . This analysis shows that newer sampling procedure can indeed sample inductive datasets that are much more similar to the original transductive graph, **greatly mitigating the PPR shortcut**.

5 Experiments

5.1 Experimental Settings

Datasets: We use the new datasets created in Section 4.1. For the (E) setting, this includes WN18RR, HetioNet, and CoDEX-M. For the (E, R) setting, it is FB15k-237 and CoDEX-M. We sample two inference graphs for each dataset, except for CoDEX-M on the (E) setting where we could only find one suitable graph for inference. For each inference graph, 10% of edges are randomly removed for testing. For validation 10% of edges are removed from the training graph. Note that while previous studies [13, 33] validate against

Table 2: Mean Δ SPD and PPR Hits@10 of new and old Inductive (“Ind.”) datasets vs. their Transductive (“Trans.”) parent. We highlight the value of the inductive dataset closer to the transductive as blue.

Task	Dataset	Mean PPR Hits@10			Mean Δ SPD		
		Trans.	Ind. Old	Ind. New	Trans.	Ind. Old	Ind. New
(E)	WN18RR	46.2	66.0	45.1	4.1	6.3	3.2
	CoDEX-M	9.0	21.1	11.2	0.2	0.78	0.24
	HetioNet	2.4	NA	2.7	0.55	NA	0.29
(E, R)	FB15k-237	2.7	21.4	10.8	0.46	2.42	0.48
	CoDEX-M	9.0	NA	13.2	0.20	NA	0.42

samples from the inference graph, it is necessary that the validation samples be extracted from the train graph. This is because using validation samples from the inference graph can be seen as a form of *test leakage*, as we are able to see the inference graph before testing. As such, because the inference graphs must remain unobserved during training, we can only sample validation from the training graph. The statistics for each dataset can be found in Appendix B.2.

Evaluation: For a given test triple (s, r, o) , we strive to predict both s and o individually. This is framed as a ranking problem where we want the probability of the correct entity (e.g., o) to rank higher than all possible negative entities. Given the rank of the true entity among the negatives, we calculate both the Hit@K and the mean reciprocal rank (MRR), using the filtered setting following [4]. Following previous work [14, 20, 41], we evaluate against all possible negative entities.

Baseline Methods: We consider prominent KGC methods including NBFNet [44], RED-GNN [41], NodePiece [13], InGram [20], DEQ-InGram [15], and Neural LP [39]. We also consider the recent foundation model ULTRA [14]. Note that we were unable to obtain results ISDEA+, as the current code only works properly when evaluating against 50 random negatives. We also omit methods that have been shown to either be prohibitively expensive (e.g., [21, 23, 33]) or require the use of textual information [8, 17].

Hyperparameters: Due to the different types and ranges of hyperparameters used for each method, the exact hyperparameters and their ranges differ by method. For each method, we tried to follow the recommended ranges used by the authors. For InGram [20] we tuned the learning rate in $\{1e^{-3}, 5e^{-4}\}$ and the number of entity layers in $\{2, 4\}$. For NodePiece [13] we tuned the learning rate from $\{1e^{-3}, 1e^{-4}\}$ and the loss margin from $\{15, 25\}$. For RED-GNN [41], we tuned the learning rate from $\{5e^{-3}, 5e^{-4}\}$ and the dropout from $\{0.1, 0.3\}$. In their experiments, NBFNet [44] uses the same hyperparameters across all datasets. We therefore do the same. For Neural LP [39] we also use the default set of hyperparameters that is shared across datasets.

Training Settings: Each model was trained on either a: Tesla V100 32Gb, NVIDIA RTX A6000 48Gb, NVIDIA RTX A5000 24Gb, or Quadro RTX 8000 48Gb. All models were implemented in PyTorch [25] and Torch-Geometric [11].

5.2 Results

Main Results: The main results for the supervised methods can be found in Tables 3 and 4. We observe that on nearly every dataset, NBFNet and RED-GNN are the two best models. This indicates

that conditional MPNNs [19], the class of model in which both belong to, are necessary for strong performance in inductive KGC. Interestingly, we observe that InGram struggles in the (E, R) setting. This is even true when the % of new relations is high. This runs counter to the results on older inductive datasets [20] where InGram excelled over NBFNet and RED-GNN. However, this is not true for DEQ-InGram, which performs consistently well under the (E, R) setting. We also observe that Neural LP sometimes fails to converge, resulting in a near zero performance and thus causing the model to have a high performance variance. Lastly, the results when evaluating via MRR can be found in Appendix A.3 and are consistent with those shown here.

Performance Comparison of PPR vs. SOTA: In our original analysis, we showed that for the older inductive datasets, the performance gap between the SOTA method of each dataset and PPR is quite small. Specifically, the mean % difference between the two was relatively small at 25-29% (see Figure 1). We now perform the same analysis on the new inductive datasets. The results are shown in Figure 6. We observe that PPR generally performs much worse than the SOTA method with a mean % difference of 101%. Furthermore, this is more in line with the transductive datasets which have a mean % difference of 121%. This suggests that in addition to the decrease in raw PPR performance, the relative performance of PPR also decreases on the newer datasets.

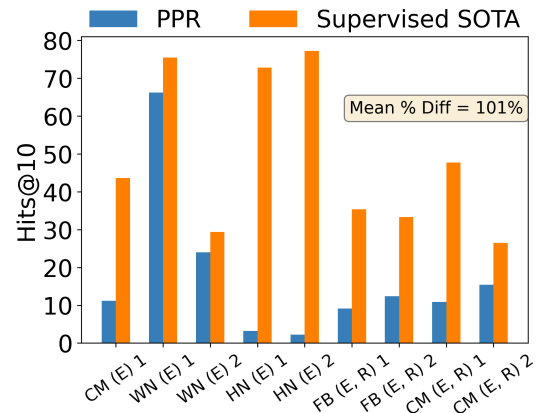
**Figure 6: PPR vs. SOTA Hits@10 on new datasets.**

Table 3: (E) Inductive Results (Hits@10) for supervised methods.

Models	CoDEX-M	WN18RR		HetioNet	
	Inference 1	Inference 1	Inference 2	Inference 1	Inference 2
PPR	11.2	66.2	24	3.2	2.2
Neural LP	13.0 ± 17.9	37.9 ± 1.4	14.8 ± 1.9	12.0 ± 16.4	10.7 ± 15.0
NodePiece	6.8 ± 0.8	29.6 ± 0.8	4.8 ± 0.6	10.2 ± 0.9	15.4 ± 0.9
InGram	20.1 ± 3.5	38.0 ± 2.4	8.0 ± 2.9	21.9 ± 1.1	22.3 ± 2.8
DEq-InGram	23.8 ± 1.6	62.5 ± 0.8	19.1 ± 3.1	26.5 ± 4.1	28.8 ± 3.5
RED-GNN	<u>35.6 ± 2.3</u>	<u>72.9 ± 0.4</u>	<u>27.7 ± 0.3</u>	68.3 ± 3.0	85.1 ± 2.7
NBFNet	43.6 ± 0.2	75.5 ± 0.2	29.4 ± 2.5	72.8 ± 3.8	<u>77.2 ± 0.4</u>

Table 4: (E, R) Inductive Results for supervised methods. The % of new relations are in parentheses.

Models	FB15k-237		CoDEX-M	
	Inference 1 (27%)	Inference 2 (63%)	Inference 1 (10%)	Inference 2 (57%)
PPR	9.1	12.4	10.9	15.4
Neural LP	17.5 ± 9.9	22.4 ± 12.8	16.7 ± 22.8	9.8 ± 13.7
NodePiece	3.0 ± 0.6	4.7 ± 0.5	3.1 ± 0.6	2.5 ± 1.0
InGram	23.8 ± 3.0	20.2 ± 2.0	20.4 ± 3.3	15.9 ± 10.0
DEq-InGram	35.4 ± 2.5	<u>27.1 ± 3.5</u>	<u>35.2 ± 14.4</u>	<u>24.7 ± 0.9</u>
RED-GNN	21.6 ± 5.8	33.3 ± 4.2	29.2 ± 2.9	26.5 ± 10.4
NBFNet	<u>27.5 ± 1.8</u>	26.2 ± 0.3	47.7 ± 11.8	17.6 ± 10.0

Table 5: Mean performance on Old vs. New inductive datasets by Method. Red indicates a decrease in the mean performance on the newer splits.

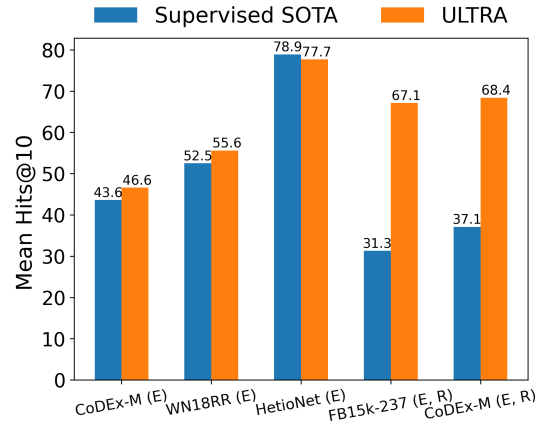
Models	WN18RR (E)			FB15k-237 (E, R)		
	Old Ind.	New Ind.	% Diff	Old Ind.	New Ind.	% Diff
PPR	66.0	45.1	-31.7%	21.4	10.8	-49.5%
Neural LP	67.6	26.4	-61.0%	16.2	20.0	+23.1%
NodePiece	29.8	17.2	-42.3%	5.0	3.9	-23.0%
InGram	49.9	23.0	-53.9%	29.6	22.0	-25.7%
RED-GNN	70.6	50.3	-28.8%	25.0	27.5	+9.8%
NBFNet	72.2	52.5	-27.4%	24.8	26.9	+8.3%
Mean	-	-	-40.6%	-	-	-9.5%

Performance Comparison on New and Old Inductive Datasets:

In Table 2, we compared both the PPR performance and Δ SPD on the new and older inductive datasets. We found that both metrics tend to be much higher on the older inductive datasets, indicating that our newer splits are effective in mitigating the shortcut. Given those results, a natural question is *whether we see a similar drop in performance for neural methods?* We limit our analysis to WN18RR (E) and FB15k-237 (E, R). This is either due to a lack of older datasets (i.e., CoDEX-M (E, R) and HetioNet (E)) or minimal results on the older datasets, i.e., CoDEX-M (E). For each dataset, we compute the mean performance across inference graphs. The results are shown in Table 5. We find that performance of most methods drops significantly on both datasets, with an average drop of 40.6% and 9.5% on WN18RR (E) and FB15k-237 (E, R), respectively. **This suggests that removing the shortcut has a large negative effect on the performance, suggesting that our new datasets are indeed harder.**

Performance of ULTRA [14]: We further compare against ULTRA, a recent foundation model designed for fully inductive KGC. We evaluate ULTRA under the 0-shot setting. Since the setting of

ULTRA differs from that of the other methods (i.e., 0-shot), we display it separately from the other methods in Tables 3 and 4. See Appendix D for more details on the versions of ULTRA used. The results are in Figure 7 where for each dataset, we average the results across the different inference graphs (full results in Appendix A.2). On the (E) task, ULTRA is comparable to the supervised SOTA. However, on the (E, R) task, ULTRA significantly outperforms other methods. This suggests that ULTRA contains a greater generalization ability than other methods.

**Figure 7: Mean Hits@10 for ULTRA vs. Supervised SOTA****6 Conclusion**

In this paper we study the problem of constructing datasets for inductive knowledge graph completion. Upon examination, we find

that we can achieve competitive performance on most inductive datasets through the use of Personalized PageRank [24], which ignores the relational structure of the graph. Through our study, we uncover that this shortcut is due to how inductive datasets are created. To remedy this problem, we propose a new dataset construction process based on graph partitioning that empirically mitigates the impact of the studied shortcut. We then construct new benchmark datasets using this new procedure and benchmark various methods. Examining the results, we observe that the relative performance decreases on most datasets and methods, indicating that the newer benchmark datasets are harder than the previous ones. For future work, we plan to explore creating inductive KG datasets that aren't sampled from existing transductive datasets.

Acknowledgments

This research is supported by the National Science Foundation (NSF) under grant numbers CNS2321416, IIS2212032, IIS2212144, IOS2107215, DUE2234015, CNS2246050, DRL2405483 and IOS2035472, US Department of Commerce, Gates Foundation, the Michigan Department of Agriculture and Rural Development, Amazon, Meta, and SNAP.

References

- [1] Farahnaz Akrami, Mohammed Samiul Saeef, Qingheng Zhang, Wei Hu, and Chengkai Li. 2020. Realistic re-evaluation of knowledge graph completion methods: An experimental study. In *Proceedings of the 2020 ACM SIGMOD International Conference on Management of Data*. 1995–2010.
- [2] Reid Andersen, Fan Chung, and Kevin Lang. 2006. Local graph partitioning using pagerank vectors. In *2006 47th Annual IEEE Symposium on Foundations of Computer Science (FOCS'06)*. IEEE, 475–486.
- [3] Vincent D Blondel, Jean-Loup Guillaume, Renaud Lambiotte, and Etienne Lefevre. 2008. Fast unfolding of communities in large networks. *Journal of statistical mechanics: theory and experiment* 2008, 10 (2008), P10008.
- [4] Antoine Bordes, Nicolas Usunier, Alberto Garcia-Duran, Jason Weston, and Oksana Yakhnenko. 2013. Translating embeddings for modeling multi-relational data. *Advances in neural information processing systems* 26 (2013).
- [5] Payal Chandak, Kexin Huang, and Marinka Zitnik. 2023. Building a knowledge graph to enable precision medicine. *Scientific Data* 10, 1 (2023), 67.
- [6] Yihong Chen, Pasquale Minervini, Sebastian Riedel, and Pontus Stenetorp. 2021. Relation Prediction as an Auxiliary Training Objective for Improving Multi-Relational Graph Representations. In *3rd Conference on Automated Knowledge Base Construction*.
- [7] Fan Chung. 2007. The heat kernel as the pagerank of a graph. *Proceedings of the National Academy of Sciences* 104, 50 (2007), 19735–19740.
- [8] Daniel Daza, Michael Cochez, and Paul Groth. 2021. Inductive entity representations from text via link prediction. In *Proceedings of the Web Conference 2021*. 798–808.
- [9] Tim Dettmers, Pasquale Minervini, Pontus Stenetorp, and Sebastian Riedel. 2018. Convolutional 2d knowledge graph embeddings. In *Proceedings of the AAAI conference on artificial intelligence*, Vol. 32.
- [10] Boyang Ding, Quan Wang, Bin Wang, and Li Guo. 2018. Improving Knowledge Graph Embedding Using Simple Constraints. In *Proceedings of the 56th Annual Meeting of the Association for Computational Linguistics (Volume 1: Long Papers)*. 110–121.
- [11] Matthias Fey and Jan E. Lenssen. 2019. Fast Graph Representation Learning with PyTorch Geometric. In *ICLR Workshop on Representation Learning on Graphs and Manifolds*.
- [12] Mikhail Galkin, Max Berrendorf, and Charles Tapley Hoyt. 2022. An open challenge for inductive link prediction on knowledge graphs. *arXiv preprint arXiv:2203.01520* (2022).
- [13] Mikhail Galkin, Etienne Denis, Jiapeng Wu, and William L. Hamilton. 2021. Node-Piece: Compositional and Parameter-Efficient Representations of Large Knowledge Graphs. In *International Conference on Learning Representations*.
- [14] Mikhail Galkin, Xinyu Yuan, Hesham Mostafa, Jian Tang, and Zhaocheng Zhu. 2023. Towards Foundation Models for Knowledge Graph Reasoning. In *The Twelfth International Conference on Learning Representations*.
- [15] Jianfei Gao, Yangze Zhou, Jincheng Zhou, and Bruno Ribeiro. 2023. Double equivariance for inductive link prediction for both new nodes and new relation types. *arXiv preprint arXiv:2302.01313* (2023).
- [16] Yuxia Geng, Jiaoyan Chen, Jeff Z Pan, Mingyang Chen, Song Jiang, Wen Zhang, and Huajun Chen. 2023. Relational message passing for fully inductive knowledge graph completion. In *2023 IEEE 39th International Conference on Data Engineering (ICDE)*. IEEE, 1221–1233.
- [17] Genet Asefa Gesese, Harald Sack, and Mehwish Alam. 2022. RAILD: Towards leveraging relation features for inductive link prediction in knowledge graphs. In *Proceedings of the 11th International Joint Conference on Knowledge Graphs*. 82–90.
- [18] Daniel Scott Himmelstein, Antoine Lizée, Christine Hessler, Leo Brueggeman, Sabrina L. Chen, Dexter Hadley, Ari Green, Pouya Khankhanian, and Sergio E Baranzini. 2017. Systematic integration of biomedical knowledge prioritizes drugs for repurposing. *Elife* 6 (2017), e26726.
- [19] Xingyue Huang, Miguel Romero, Ismail Ceylan, and Pablo Barceló. 2024. A Theory of Link Prediction via Relational Weisfeiler-Leman on Knowledge Graphs. *Advances in Neural Information Processing Systems* 36 (2024).
- [20] Jaemin Lee, Chanyoung Chung, and Joyce Jiyoung Whang. 2023. InGram: Inductive knowledge graph embedding via relation graphs. In *International Conference on Machine Learning*. PMLR, 18796–18809.
- [21] Shuwen Liu, Bernardo Grau, Ian Horrocks, and Egor Kostylev. 2021. Indigo: Gnn-based inductive knowledge graph completion using pair-wise encoding. *Advances in Neural Information Processing Systems* 34 (2021), 2034–2045.
- [22] Farzaneh Mahdisoltani, Joanna Biega, and Fabian M Suchanek. 2013. Yago3: A knowledge base from multilingual wikipeidias. In *CIDR*.
- [23] Sijie Mai, Shuangjia Zheng, Yuedong Yang, and Haifeng Hu. 2021. Communicative Message Passing for Inductive Relation Reasoning. In *Proceedings of the AAAI Conference on Artificial Intelligence*, Vol. 35. 4294–4302.
- [24] Lawrence Page, Sergey Brin, Rajeev Motwani, and Terry Winograd. 1999. *The PageRank citation ranking: Bringing order to the web*. Technical Report. Stanford InfoLab.
- [25] Adam Paszke, Sam Gross, Francisco Massa, Adam Lerer, James Bradbury, Gregory Chanan, Trevor Killeen, Zeming Lin, Natalia Gimelshein, Luca Antiga, Alban Desmaison, Andreas Kopf, Edward Yang, Zachary DeVito, Martin Raison, Alykhan Tejani, Sasank Chilamkurthy, Benoit Steiner, Lu Fang, Junjie Bai, and Soumith Chintala. 2019. PyTorch: An Imperative Style, High-Performance Deep Learning Library. In *Advances in Neural Information Processing Systems* 32, H. Wallach, H. Laroche, A. Beygelzimer, F. d'Alché-Buc, E. Fox, and R. Garnett (Eds.). Curran Associates, Inc., 8024–8035.
- [26] Ali Sadeghian, Mohammadreza Armandpour, Patrick Ding, and Daisy Zhe Wang. 2019. Drum: End-to-end differentiable rule mining on knowledge graphs. *Advances in Neural Information Processing Systems* 32 (2019).
- [27] Tara Safavi and Danai Koutra. 2020. CoDEX: A Comprehensive Knowledge Graph Completion Benchmark. In *Proceedings of the 2020 Conference on Empirical Methods in Natural Language Processing (EMNLP)*. 8328–8350.
- [28] Michael Schlichtkrull, Thomas N Kipf, Peter Bloem, Rianne Van Den Berg, Ivan Titov, and Max Welling. 2018. Modeling relational data with graph convolutional networks. In *European semantic web conference*. Springer, 593–607.
- [29] Jianbo Shi and Jitendra Malik. 2000. Normalized cuts and image segmentation. *IEEE Transactions on pattern analysis and machine intelligence* 22, 8 (2000), 888–905.
- [30] Harry Shomer, Wei Jin, Wentao Wang, and Jiliang Tang. 2023. Toward degree bias in embedding-based knowledge graph completion. In *Proceedings of the ACM Web Conference 2023*. 705–715.
- [31] Harry Shomer, Yao Ma, Juanhui Li, Bo Wu, Charu Aggarwal, and Jiliang Tang. 2023. Distance-Based Propagation for Efficient Knowledge Graph Reasoning. In *Proceedings of the 2023 Conference on Empirical Methods in Natural Language Processing*. 14692–14707.
- [32] Zhiqing Sun, Zhi-Hong Deng, Jian-Yun Nie, and Jian Tang. 2019. RotatE: Knowledge Graph Embedding by Relational Rotation in Complex Space. In *International Conference on Learning Representations*.
- [33] Komal Teru, Etienne Denis, and Will Hamilton. 2020. Inductive relation prediction by subgraph reasoning. In *International Conference on Machine Learning*. PMLR, 9448–9457.
- [34] Kristina Toutanova and Danqi Chen. 2015. Observed versus latent features for knowledge base and text inference. In *Proceedings of the 3rd workshop on continuous vector space models and their compositionality*. 57–66.
- [35] Théo Trouillon, Johannes Welbl, Sebastian Riedel, Éric Gaussier, and Guillaume Bouchard. 2016. Complex embeddings for simple link prediction. In *International conference on machine learning*. PMLR, 2071–2080.
- [36] Xiang Wang, Tinglin Huang, Dingxian Wang, Yancheng Yuan, Zhengguang Liu, Xiangnan He, and Tat-Seng Chua. 2021. Learning intents behind interactions with knowledge graph for recommendation. In *Proceedings of the web conference 2021*. 878–887.
- [37] Wenhan Xiong, Thien Hoang, and William Yang Wang. 2017. DeepPath: A Reinforcement Learning Method for Knowledge Graph Reasoning. In *Proceedings of the 2017 Conference on Empirical Methods in Natural Language Processing*. 564–573.

- [38] Xiaohan Xu, Peng Zhang, Yongquan He, Chengpeng Chao, and Chaoyang Yan. 2022. Subgraph neighboring relations infomax for inductive link prediction on knowledge graphs. *arXiv preprint arXiv:2208.00850* (2022).
- [39] Fan Yang, Zhilin Yang, and William W Cohen. 2017. Differentiable learning of logical rules for knowledge base reasoning. *Advances in neural information processing systems* 30 (2017).
- [40] Xiangxiang Zeng, Xinqi Tu, Yuansheng Liu, Xiangzheng Fu, and Yansen Su. 2022. Toward better drug discovery with knowledge graph. *Current opinion in structural biology* 72 (2022), 114–126.
- [41] Yongqi Zhang and Quanming Yao. 2022. Knowledge graph reasoning with relational digraph. In *Proceedings of the ACM Web Conference 2022*. 912–924.
- [42] Yongqi Zhang, Zhanke Zhou, Quanming Yao, Xiaowen Chu, and Bo Han. 2023. AdaProp: Learning Adaptive Propagation for Graph Neural Network based Knowledge Graph Reasoning. In *KDD*.
- [43] Zhaocheng Zhu, Xinyu Yuan, Michael Galkin, Louis-Pascal Khonneux, Ming Zhang, Maxime Gazeau, and Jian Tang. 2023. A* net: A scalable path-based reasoning approach for knowledge graphs. *Advances in Neural Information Processing Systems* 36 (2023), 59323–59336.
- [44] Zhaocheng Zhu, Zuobai Zhang, Louis-Pascal Khonneux, and Jian Tang. 2021. Neural bellman-ford networks: A general graph neural network framework for link prediction. *Advances in Neural Information Processing Systems* 34 (2021), 29476–29490.

A Additional Results

A.1 Supervised SOTA vs. PPR Performance

In this section we show the performance in terms of Hits@10 for the SOTA supervised method vs. the Personalized PageRank (PPR) score. We further include the % difference in performance and which method is considered SOTA. These are shown in Tables 6, 7, and 8 for the (E), (E, R), and transductive datasets, respectively. For an overview of SOTA performance on additional KG datasets, please see [14].

Table 6: Hits@10 for PPR vs. Supervised SOTA on the (E) Inductive Datasets

Dataset	Supervised SOTA	PPR	% Difference	SOTA Method
WN v1	82.6	77.1	7%	NBFNet [44]
WN v2	79.8	74.4	12%	NBFNet [44]
WN v3	56.8	45.2	26%	NBFNet [44]
WN v4	74.3	67.3	10%	A*Net [43]
FB v1	60.7	41.2	47%	NBFNet [44]
FB v2	70.4	47.6	48%	NBFNet [31]
FB v3	66.7	43.5	53%	NBFNet [44]
FB v4	66.8	38.4	74%	NBFNet [44]
ILPC-S	25.1	19.8	27%	NodePiece [13]
ILPC-L	14.6	22.5	-35%	NodePiece [13]

Table 7: Hits@10 for PPR vs. Supervised SOTA on the (E, R) Inductive Datasets

Dataset	Supervised SOTA	PPR	% Difference	SOTA Method
FB-100	37.1	22.2	67%	InGram [20]
FB-75	32.5	21.9	48%	InGram [20]
FB-50	21.8	20.5	6%	InGram [20]
FB-25	27.1	20.9	30%	InGram [20]
WK-100	16.9	15.8	7%	InGram [20]
WK-75	36.2	29.5	23%	InGram [20]
WK-50	13.5	10.6	27%	InGram [20]
WK-25	30.9	23.2	33%	InGram [20]

A.2 Performance of ULTRA

We include the full results of ULTRA [14] on each dataset and inference graph. The result on the (E) datasets are in Table 9 while those for the (E, R) datasets are in Table 10.

Table 9: (E) Inductive Results for ULTRA [14]

Dataset	Graph	Hits@10	MRR
CoDEx-M	Inference 1	30.2	46.6
WN18RR	Inference 1	64.7	72.7
	Inference 2	21.4	38.5
HetioNet	Inference 1	57.9	69.1
	Inference 2	72.7	86.3

Table 10: (E) Inductive Results for ULTRA [14]

Metric	FB15k-237		CoDEx-M	
	Inference 1	Inference 2	Inference 1	Inference 2
MRR	45.7	38	30.4	73.7
Hits@10	69.6	64.5	45.7	91.3

Table 11: Performance of Tail Degree [30], PPR, and SOTA method. Performance is in terms of Hits@10. We further bold the larger of the PPR and tail degree performance.

Task	Dataset	Tail Degree	PPR	SOTA
Inductive	WN v1	10.4	77.1	82.6
	WN v2	5.1	74.4	83.6
	WN v3	10.1	45.2	58.2
	WN v4	2.2	67.3	74.5
	FB v1	20.5	41.2	60.7
	FB v2	22.7	47.6	70.4
	FB v3	16.8	43.5	67.7
	FB v4	16.1	38.4	66.8
Transductive	WN18RR	2.0	46.2	59.9
	FB15k-237	6.0	2.7	66.6
	DBPedia100k	2.9	30.2	41.8

A.3 MRR Performance

We further include the performance on the new datasets when evaluating via MRR. The results are shown in Tables 12 and 13 for the (E) and (E, R) results, respectively. We can observe that these results are highly consistent when evaluating via Hits@10. That is, under the (E) setting both NBFNet and RED-GNN perform best, while under the (E, R) setting DEq-InGram also excels. This suggests that our observations hold under multiple evaluation metrics.

Table 8: Hits@10 for PPR vs. Supervised SOTA on the Transductive Datasets

Dataset	Supervised SOTA	PPR	% Difference	SOTA Method
FB15k-237	66.6	2.7	2367%	NBF+TAGNet [31]
WN18RR	59.9	46.2	30%	NBF+TAGNet [31]
CoDEx-M	49.0	9.0	444%	ComplEx RP [6]
CoDEx-S	66.3	8.6	671%	ComplEx RP [6]
CoDEx-L	47.3	9.0	426%	ComplEx RP [6]
Hetionet	40.3	2.4	1579%	RotatE [32]
DBPedia100k	41.8	30.2	38%	ComplEx-NNE+AER [10]

Table 12: (E) Inductive Results (MRR) for supervised methods.

Models	CoDEx-M	WN18RR		HetioNet	
	Inference 1	Inference 1	Inference 2	Inference 1	Inference 2
PPR	3.3	25.6	7.9	2.3	2.1
Neural LP	9.2 ± 11.2	23.9 ± 2.0	10.5 ± 1.8	7.3 ± 9.9	6.7 ± 9.3
NodePiece	3.1 ± 0.3	20.6 ± 0.8	3.3 ± 0.4	5.1 ± 0.6	7.2 ± 0.6
InGram	10.1 ± 1.5	15.9 ± 0.7	3.8 ± 1.1	11.2 ± 0.5	11.5 ± 2.1
DEq-InGram	11.2 ± 0.6	25.4 ± 0.5	9.8 ± 1.7	16.5 ± 2.9	16.9 ± 2.0
RED-GNN	<u>22.1 ± 1.8</u>	67.8 ± 0.5	<u>16.4 ± 1.3</u>	53.8 ± 2.5	68.6 ± 4.3
NBFNet	27.6 ± 0.2	<u>66.6 ± 0.1</u>	17.6 ± 0.1	<u>39.1 ± 1.2</u>	<u>45.2 ± 0.5</u>

Table 13: (E, R) Inductive Results (MRR) for supervised methods. The % of new relations are in parentheses.

Models	FB15k-237		CoDEx-M	
	Inference 1 (27%)	Inference 2 (63%)	Inference 1 (10%)	Inference 2 (57%)
PPR	3.8	4.7	3.3	7.1
Neural LP	8.8 ± 4.9	11.3 ± 6.6	13.8 ± 18.8	7.4 ± 9.4
NodePiece	1.4 ± 0.1	2.6 ± 0.2	1.5 ± 0.2	1.6 ± 0.4
InGram	11.2 ± 1.9	9.2 ± 0.9	10.3 ± 1.2	7.2 ± 4.2
DEq-InGram	19.5 ± 2.0	13.4 ± 1.2	<u>18.7 ± 7.6</u>	<u>13.0 ± 1.3</u>
RED-GNN	11.8 ± 2.8	<u>19.8 ± 2.2</u>	16.8 ± 1.6	14.7 ± 5.3
NBFNet	<u>15.8 ± 0.9</u>	15.9 ± 0.2	27.9 ± 8.8	8.5 ± 4.8

A.4 Performance of Other Potential Shortcuts

In our study, we show that PPR can achieve strong performance on most inductive KG datasets, indicating a shortcut. A natural question is whether this is true for just PPR, or if other shortcuts exist. Another bias discussed in KG literature is degree bias [30]. In their study, they show that that KG methods tend to perform better on entities with a higher degree. Specifically, they observe that what matters is the degree of the entity being predicted (they refer to this as the “tail degree”). Based on this, we study whether the tail degree can be a good predictor of performance.

We show that results on a number of inductive and transductive datasets in Table 11. We report Hits@10 for all results. We find that the tail degree often achieves a much lower performance than PPR. Specifically, for the datasets in Table 11, while the PPR performance is on average only 31% lower than the SOTA, the tail degree performance is 84% lower. This indicates the severity of the PPR shortcut is much more severe as compared to other known biases like the tail degree.

B Datasets

B.1 Existing Datasets

We detail the statistics of all existing transductive and inductive datasets in Tables 14, 15, and 16, respectively. Note that we omit YAGO3-10 [22] as [1] show that the dataset is dominated by two duplicate relations, making most triples trivial to classify. Also, we omit NELL-995 and any inductive datasets derived from it due to findings by [27] that show that most triples in the dataset are either too generic or meaningless.

B.2 New Datasets

We further detail the statistics of all the new datasets in Tables 17 and 18.

C Inductive Generation Experiments

We give more details on the experiments conducted in Section 3.3 and shown in Figures 4. Given the transductive dataset FB15k-237 [34], we generate a number of different inductive datasets using the common procedure used by [20, 33]. We describe this procedure

Table 14: Statistics for Transductive Datasets.

Dataset	#Entities	#Relations	#Train	#Validation	#Test
FB15k-237 [34]	14,541	237	272,115	17,535	20,466
WN18RR [9]	40,943	11	86,835	3,034	3,134
CoDEX-S [27]	2,034	42	32,888	1,827	1,828
CoDEX-M [27]	17,050	51	185,584	10,310	10,311
CoDEX-L [27]	77,951	69	551,193	30,622	30,622
HetioNet [18]	45,158	24	2,025,177	112,510	112,510
DBpedia100k [10]	99,604	470	597,572	50,000	50,000

Table 15: Statistics for (E) Inductive Datasets.

Dataset	#Relations	Train Graph		Validation Graph			Test Graph		
		#Entities	#Triples	#Entities	#Triples	#Valid	#Entities	#Triples	#Test
FB15k-237 v1 [33]	180	1,594	4,245	1,594	4,245	489	1,093	1,993	205
FB15k-237 v2 [33]	200	2,608	9,739	2,608	9,739	1,166	1,660	4,145	478
FB15k-237 v3 [33]	215	3,668	17,986	3,668	17,986	2,194	2,501	7,406	865
FB15k-237 v4 [33]	219	4,707	27,203	4,707	27,203	3,352	3,051	11,714	1,424
WN18RR v1 [33]	9	2,746	5,410	2,746	5,410	630	922	1,618	188
WN18RR v2 [33]	10	6,954	15,262	6,954	15,262	1,838	2,757	4,011	441
WN18RR v3 [33]	11	12,078	25,901	12,078	25,901	3,097	5,084	6,327	605
WN18RR v4 [33]	9	3,861	7,940	3,861	7,940	934	7,084	12,334	1,429
ILPC-S [12]	48	10,230	78,616	6,653	20,960	2,908	6,653	20,960	2902
ILPC-L [12]	65	46,626	202,446	29,246	77,044	10,179	29,246	77,044	10,184

Table 16: Statistics for (E, R) Inductive Datasets.

Dataset	Train Graph			Validation Graph				Test Graph			
	#Entities	#Rels	#Triples	#Entities	#Rels	#Triples	#Valid	#Entities	#Rels	#Triples	#Test
FB-25 [20]	5,190	163	91,571	4,097	216	17,147	5,716	4,097	216	17,147	5,716
FB-50 [20]	5,190	153	85,375	4,445	205	11,636	3,879	4,445	205	11,636	3,879
FB-75 [20]	4,659	134	62,809	2,792	186	9,316	3,106	2,792	186	9,316	3,106
FB-100 [20]	4,659	134	62,809	2,624	77	6,987	2,329	2,624	77	6,987	2,329
WK-25 [20]	12,659	47	41,873	3,228	74	3,391	1,130	3,228	74	3,391	1,131
WK-50 [20]	12,022	72	82,481	9,328	93	9,672	3,224	9,328	93	9,672	3,225
WK-75 [20]	6,853	52	28,741	2,722	65	3,430	1,143	2,722	65	3,430	1,144
WK-100 [20]	9,784	67	49,875	12,136	37	13,487	4,496	12,136	37	13,487	4,496

Table 17: Statistics for New (E) Inductive Datasets.

Dataset	Graph	# Edges	# Entities	# Rels	# Valid/Test	Δ SPD
CoDEX-M	Train	76,960	8,362	47	8,552	NA
	Inference 1	69,073	8,003	40	7,674	0.24
WN18RR	Train	24,584	12,142	11	2,458	NA
	Inference 1	18,258	8,660	10	1,831	4.87
	Inference 2	5,838	2,975	8	572	1.47
HetioNet	Train	101,667	3,971	14	11,271	NA
	Inference 1	49,590	2,279	11	5,490	0.38
	Inference 2	37,927	2,455	12	4,187	0.19

Table 18: Statistics for New (E, R) Inductive Datasets.

Dataset	Graph	# Edges	# Entities	# Rels	# Valid/Test	% New Rels	Δ SPD
FB15k-237	Train	45,597	2,864	104	5,062	NA	NA
	Inference 1	35,937	1,835	72	3,898	62.8%	0.63
	Inference 2	51,693	2,606	143	5,735	27.1%	0.34
CoDEX-M	Train	29,634	4,038	36	3293	NA	NA
	Inference 1	70,137	7,938	39	7,794	9.9%	0.24
	Inference 2	8,821	474	28	979	56.8%	0.60

Table 19: FB15k-237 - Inductive Generative Experiments Configurations. Results are over 3 Random Seeds.

# Train Ents	# Inf. Ents	Max Train	Max Inf.	# Train Edges	# Test Edges	Δ SPD	PPR Hits@10
10	20	10	50	7,599	72,688	1.14	0.166
10	20	15	50	18,518	49,057	1.31	0.180
10	20	25	50	43,077	36,054	1.46	0.213
10	20	50	50	91,843	18,370	1.71	0.309
10	20	100	50	129,782	15,179	1.72	0.235
10	20	50	10	91,843	4,304	2.15	0.400
10	20	50	25	91,843	13,374	1.79	0.319
10	20	50	50	91,843	18,370	1.71	0.309
10	20	50	100	91,843	21,512	1.71	0.310
10	20	50	50	91,843	18,370	1.71	0.309
20	20	50	50	149,635	8,258	2.38	0.317
40	20	50	50	210,109	973	3.89	0.408
10	10	50	50	91,843	11,177	1.6	0.325
10	20	50	50	91,843	18,370	1.71	0.309
10	40	50	50	91,843	36,353	1.81	0.266
10	80	50	50	91,843	47,419	1.83	0.254
10	160	50	50	91,843	55,233	1.93	0.259

in detail in Section 2. Note that for simplicity, we only created datasets for the (E) inductive task. However, the same conclusions should hold for (E, R). Lastly, we only create one graph for inference as is done in previous work.

We generate the inductive datasets by modifying the following set of parameters:

- **# of Initial Train Entities:** This is the number of entities that are first assigned to the train graph.
- **# of Initial Inference Entities:** This is the number of entities that are first assigned to the inference graph.
- **Max Train Neighborhood Size:** We extract the 2-hop neighborhood for each of the initial train entities. To avoid exponential growth, we limit the number of entities selected in each hop to 50. For example, if node 1 has 30 1-hop neighbors and 120 2-hop neighbors, then $30 + 50 = 80$ entities are added through the expansion of node 1.
- **Max Inference Neighborhood Size:** This follows the same logic as for train but for inference.

The default neighborhood size is set to 50 for the inductive datasets created by [33] and [20]. For [20] they consider 10 and 20, initial entities for train and inference, respectively. This information is not reported for [33].

To simulate the effect of the different parameter values, we create inductive datasets by using a number of different combinations of parameters. For each parameter, we modify it while holding the others constant. This allows us to explore the effect of just that variable. It allows us to avoid running an excessive amount of experiments. The default values are those used in [20] and noted above. In total, there are 17 parameter configurations. For each parameter configuration, we create 3 different datasets through the use of 3 different random seeds. This results in a total of 51 inductive datasets. We then evaluate the performance of PPR on each inference graph and calculate the Δ SPD. The results for those datasets with the same configuration are then averaged together. All possible configurations and their resulting mean statistics can be

found in Table 19. These results are visualized in the main content in Figures 4.

D ULTRA Settings

When evaluating ULTRA [14] we use the 0-shot setting. By default, we use the checkpoint they provided that was trained on the transductive datasets: FB15k-237 [34], WN18RR [9], CoDEx-M [27], and NELL-995 [37]. However, since we create our own inductive splits from FB15k-237, CoDEx-M, and WN18RR, there is risk of test leakage. That is, some triples that may have been in the transductive training graph, may now be a test sample in one of our splits. This gives ULTRA an unfair advantage as it has already seen that triple.

To combat this issue, we train three different versions of ULTRA that omits the transductive dataset used to create that specific inductive dataset. This includes:

- *w/o FB15k-237:* Trained using WN18RR, CoDEx-M, and NELL-995.
- *w/o WN18RR:* Trained using FB15k-237, CoDEx-M, and NELL-995.
- *w/o CoDEx-M:* Trained using FB15k-237, WN18RR, and NELL-995.

We follow the same settings used to train the original checkpoints provided by the authors of ULTRA. Lastly, since HetioNet is not one of the four datasets used, no additional model is needed.

The results are shown in Table 22, where the “W/o” column represents the results when removing the parent transductive dataset and “With” corresponds to the original pre-trained checkpoint provided by the authors of ULTRA [14]. In practice, we observe a small but noteworthy decrease in performance when removing the offending transductive dataset from the pre-trained model.

E Analysis of the WikiTopics and PediaTypes Datasets

We further include an analysis of the WikiTopics and PediaTypes inductive datasets introduced by Gao et al. [15]. For these datasets,

Table 20: PPR Performance on PediaTypes [15] datasets.

Dataset	50 Negatives			All Negatives	Δ SPD
	Neural Hits@10	PPR Hits@10	% Difference	PPR Hits@10	
EN-FR	95.4%	96.0%	-0.6%	44.1%	2.7
FR-EN	90.6%	96.2%	-5.8%	48.1%	2.3
EN-DE	97.7%	93.9%	4.0%	34.7%	2.1
DE-EN	95.0%	90.6%	4.9%	20.8%	1.6
DB-WD	86.6%	76.4%	13.4%	23.5%	0.6
WD-DB	91.5%	92.0%	-0.5%	42.9%	2.5
DB-YG	71.5%	76.9%	-7.0%	15.2%	2.7
YG-DB	80.5%	85.1%	-5.4%	30.7%	3.5

Table 21: PPR Performance on WikiTopics [15] datasets.

Dataset	50 Negatives			All Negatives	Δ SPD
	Neural Hits@10	PPR Hits@10	% Difference	PPR Hits@10	
Art	92.3%	79.3%	16.4%	14.7%	1.1
Award	93.6%	95.8%	-2.3%	24.2%	3.4
Edu	97.0%	72.4%	34.0%	20.8%	2.7
Health	98.9%	91.5%	8.1%	59.6%	3.3
Infra	97.8%	97.2%	0.6%	61.4%	5.4
Sci	96.7%	84.3%	14.7%	25.5%	4.4
Sport	81.2%	82.9%	-2.1%	14.4%	0.3
Tax	93.7%	64.1%	46.1%	29.0%	0.8
Loc	N/A	96.5%	N/A	74.1%	1.4
Org	N/A	94.0%	N/A	8.9%	2.8
People	N/A	94.9%	N/A	64.6%	2.7

Table 22: Performance (Hits@10) of ULTRA when pre-trained and w/o the parent transductive dataset. Note that this doesn't apply to HetioNet.

Dataset	Inference Graph	W/o	With	% Difference
CoDEX-M (E)	1	46.6	50.2	-7.2%
WN18RR (E)	1	71.9	72.7	+1.1%
	2	38.8	38.5	-0.8%
FB15k-237 (E, R)	1	69.6	72.1	-4.5%
	2	64.5	64.8	-0.5%
CoDEX-M (E, R)	1	45.7	50.4	-9.3%
	2	91.1	91.3	-0.2%

the train and inference graphs contain completely separate entities and relations. For each dataset we record the **(a)** Neural SOTA performance (taken from [15]), **(b)** PPR performance, **(c)** % difference in performance, and **(d)** Δ SPD. In their original study, Gao et al. [15] use 50 random negatives during evaluation, instead of all negative entities used in ours. To account for this, we compute the PPR performance using both evaluation settings. The results for the PediaTypes and WikiTopics datasets are in Tables 20 and 21, respectively.

From the results we can make multiple observations. First, PPR performs well under both settings. Under the all negatives setting, the mean PPR performance is 32.5% and 38.3% on PediaTypes and

WikiTopics, respectively. Second, under 50 negatives, there is little difference in the PPR and Neural performance. Specifically, the % difference in performance is 0.4% and 14.2%, respectively, on PediaTypes and WikiTopics. This suggests that neural methods can only slightly outperform PPR under this setting. Lastly, the Δ SPD is high on both sets of datasets. This further corroborates our findings in Section 3.

This analysis shows that the WikiTopics and PediaTopics datasets introduced by Gao et al. [15] fall prey to the same shortcut found in other inductive datasets studied in Section 3.